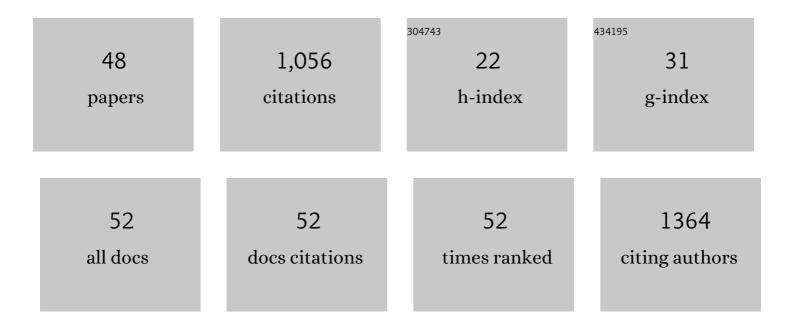
Katharina Marquardt

List of Publications by Year in descending order

Source: https://exaly.com/author-pdf/5231253/publications.pdf Version: 2024-02-01



#	Article	IF	CITATIONS
1	Metallic lead nanospheres discovered in ancient zircons. Proceedings of the National Academy of Sciences of the United States of America, 2015, 112, 4958-4963.	7.1	68
2	Experimental partitioning of F and Cl between olivine, orthopyroxene and silicate melt at Earth's mantle conditions. Chemical Geology, 2015, 416, 65-78.	3.3	62
3	First evidence of hydrous silicic fluid films around solid inclusions in gem-quality diamonds. Lithos, 2016, 260, 384-389.	1.4	61
4	Evidence for H2O-bearing fluids in the lower mantle from diamond inclusion. Lithos, 2016, 265, 237-243.	1.4	57
5	Experimental determination of melt interconnectivity and electrical conductivity in the upper mantle. Earth and Planetary Science Letters, 2017, 463, 286-297.	4.4	44
6	Role of inclination dependence of grain boundary energy on the microstructure evolution during grain growth. Acta Materialia, 2020, 188, 641-651.	7.9	42
7	New constraints on upper mantle creep mechanism inferred from silicon grain-boundary diffusion rates. Earth and Planetary Science Letters, 2016, 433, 350-359.	4.4	41
8	Seismically invisible water in Earth's transition zone?. Earth and Planetary Science Letters, 2018, 498, 9-16.	4.4	40
9	Experimental partitioning of halogens and other trace elements between olivine, pyroxenes, amphibole and aqueous fluid at 2ÂGPa and 900–1,300°C. Contributions To Mineralogy and Petrology, 2013, 166, 639-653.	3.1	39
10	The effect of water on intergranular mass transport: new insights from diffusion-controlled reaction rims in the MgO–SiO2 system. Contributions To Mineralogy and Petrology, 2012, 164, 1-16.	3.1	38
11	The structure and composition of olivine grain boundaries: 40 years of studies, status and current developments. Physics and Chemistry of Minerals, 2018, 45, 139-172.	0.8	37
12	Elastic properties of MgO nanocrystals and grain boundaries at high pressures by Brillouin scattering. Physical Review B, 2011, 84, .	3.2	33
13	Compressional pathways of $\hat{i}\pm$ -cristobalite, structure of cristobalite X-I, and towards the understanding of seifertite formation. Nature Communications, 2017, 8, 15647.	12.8	33
14	Grain boundary and volume diffusion experiments in yttrium aluminium garnet bicrystals at 1,723ÂK: a miniaturized study. Contributions To Mineralogy and Petrology, 2011, 162, 739-749.	3.1	32
15	Synthesis of [Fe(L)(bipy)] _n spin crossover nanoparticles using blockcopolymer micelles. Nanoscale, 2016, 8, 19058-19065.	5.6	30
16	Quantitative electron backscatter diffraction (EBSD) data analyses using the dictionary indexing (DI) approach: Overcoming indexing difficulties on geological materials. American Mineralogist, 2017, 102, 1843-1855.	1.9	30
17	TEXTURE AND COMPOSITION OF Pb-BEARING PYRITE FROM THE COKA MARIN POLYMETALLIC DEPOSIT, SERBIA, CONTROLLED BY NANOSCALE INCLUSIONS. Canadian Mineralogist, 2012, 50, 1-20.	1.0	29
18	Atomic structures and energies of grain boundaries in Mg2SiO4 forsterite from atomistic modeling. Physics and Chemistry of Minerals, 2012, 39, 749-760.	0.8	28

#	Article	IF	CITATIONS
19	Focused ion beam preparation and characterization of single-crystal samples for high-pressure experiments in the diamond-anvil cell. American Mineralogist, 2012, 97, 299-304.	1.9	26
20	The most frequent interfaces in olivine aggregates: the GBCD and its importance for grain boundary related processes. Contributions To Mineralogy and Petrology, 2015, 170, 1.	3.1	26
21	Mg lattice diffusion in iron-free olivine and implications to conductivity anomaly in the oceanic asthenosphere. Earth and Planetary Science Letters, 2018, 484, 204-212.	4.4	24
22	Synthetic near Σ5 (210)/[100] grain boundary in YAG fabricated by direct bonding: structure and stability. Physics and Chemistry of Minerals, 2010, 37, 291-300.	0.8	22
23	Degradation mechanisms of SiC/BN/SiC after low temperature humidity exposure. Journal of the European Ceramic Society, 2020, 40, 3863-3874.	5.7	20
24	Nitrogen nanoinclusions in milky diamonds from Juina area, Mato Grosso State, Brazil. Lithos, 2016, 265, 57-67.	1.4	17
25	Intragranular plasticity vs. grain boundary sliding (GBS) in forsterite: Microstructural evidence at high pressures (3.5–5.0 GPa). American Mineralogist, 2019, 104, 220-231.	1.9	15
26	Volume diffusion of Ytterbium in YAG: thin-film experiments and combined TEM–RBS analysis. Physics and Chemistry of Minerals, 2010, 37, 751-760.	0.8	14
27	The effect of crystallite size and stress condition on the equation of state of nanocrystalline MgO. Journal of Applied Physics, 2011, 110, .	2.5	14
28	Diffusion in yttrium aluminium garnet at the nanometer-scale: Insight into the effective grain boundary width. American Mineralogist, 2011, 96, 1521-1529.	1.9	13
29	Structural insights and elasticity of single-crystal antigorite from high-pressure Raman and Brillouin spectroscopy measured in the (010) plane. American Mineralogist, 2015, 100, 1932-1939.	1.9	11
30	Multi-sample loading technique for comparative physical property measurements in the diamond-anvil cell. High Pressure Research, 2017, 37, 159-169.	1.2	11
31	Weathering of Bi-bearing tennantite. Chemical Geology, 2018, 499, 1-25.	3.3	11
32	The Effect of Grain Boundaries on Plastic Deformation of Olivine. Journal of Geophysical Research: Solid Earth, 2021, 126, e2020JB020273.	3.4	11
33	STEM EDX Nitrogen Mapping of Nanoinclusions in Milky Diamonds from Juina, Brazil, Using a Windowless Silicon Drift Detector System. Analytical Chemistry, 2016, 88, 5804-5808.	6.5	9
34	Experimental study on the pseudobinary H2O+NaAlSi3O8 at 600–800°C and 0.3–2.4GPa. Chemical Geology, 2014, 388, 40-47.	3.3	8
35	Evidence for complex iron oxides in the deep mantle from FeNi(Cu) inclusions in superdeep diamond. Proceedings of the National Academy of Sciences of the United States of America, 2020, 117, 21088-21094.	7.1	8
36	Location and quantification of hydrogen in Ca- and Sr-anorthite. European Journal of Mineralogy, 2010, 22, 103-112.	1.3	7

#	Article	IF	CITATIONS
37	Pressure, temperature, water content, and oxygen fugacity dependence of the Mg grain-boundary diffusion coefficient in forsterite. American Mineralogist, 2018, 103, 1354-1361.	1.9	7
38	P-T-X-controlled element transport through granulite-facies ternary feldspar from Lofoten, Norway. Contributions To Mineralogy and Petrology, 2008, 156, 359-375.	3.1	6
39	Anisotropy of self-diffusion in forsterite grain boundaries derived from molecular dynamics simulations. Contributions To Mineralogy and Petrology, 2016, 171, 1.	3.1	6
40	Grain boundary diffusion and its relation to segregation of multiple elements in yttrium aluminum garnet. European Journal of Mineralogy, 2020, 32, 675-696.	1.3	6
41	Lead diffusion in CaTiO3: A combined study using Rutherford backscattering and TOF-SIMS for depth profiling to reveal the role of lattice strain in diffusion processes. American Mineralogist, 2019, 104, 557-568.	1.9	5
42	Realizing shape and size control for the synthesis of coordination polymer nanoparticles templated by diblock copolymer micelles. Nanoscale, 2022, 14, 3131-3147.	5.6	4
43	Optimized FIB Sample Preparation for Atomic Resolution Analytical STEM at Low kV - A Key Requirement for Successful Application. Microscopy and Microanalysis, 2011, 17, 630-631.	0.4	3
44	Silicic microinclusions in a metasomatized eclogite from Roberts Victor mine, South Africa. Lithos, 2021, 388-389, 106057.	1.4	3
45	A transmission x-ray microscopy and NEXAFS approach for studying corroded silicate glasses at the nanometre scale. Journal of Commonwealth Law and Legal Education, 2018, 59, 11-26.	0.5	2
46	Magnesium transport in olivine mantle: new insights from miniaturized study of volume and grain boundary diffusion in Mg2SiO4 bi-crystals. Contributions To Mineralogy and Petrology, 2021, 176, 1.	3.1	2
47	A reversed redox gradient in Earth's mantle transition zone. Earth and Planetary Science Letters, 2021, 575, 117181.	4.4	1
48	Accurate Grain and Phase Boundary Location by Dictionary-based Indexing of Geological EBSD Data. Microscopy and Microanalysis, 2017, 23, 2156-2157.	0.4	0